Dicle University
Journal of Engineering
https://dergipark.org.tr/tr/pub/dumf
duje.dicle.edu.tr

Research Article

Design and implementation of multiband microstrip antenna for energy harvesting

Muhammed SÜZGÜN[1], Mustafa CANSIZ[2]*

1 Dicle University, Department of Electrical and Electronics Engineering, Diyarbakır, Turkey, msuzgun96@gmail.com, ORCID: https://orcid.org/0009-0009-6663-3920

2 Dicle University, Department of Electrical and Electronics Engineering, Diyarbakır, Turkey, mustafa.cansiz@dicle.edu.tr, ORCID: https://orcid.org/0000-0003-2534-9770

ARTICLE INFO

Article history:

Received 21 February 2024
Received in revised form 2 June 2024
Accepted 4 July 2024
Available online 30 September 2024

Keywords:

Microstrip antenna, Antenna design, Multiband, RF signal, Energy harvesting

Doi: 10.24012/dumf.1440939

* Corresponding author

ABSTRACT

Antennas are of great importance in energy harvesting systems. It is possible to collect more energy with RF energy harvesting systems by using multiband antennas. In this study, a microstrip antenna was designed and fabricated for operation at 307 MHz, 1721 MHz, and 5447 MHz carrier frequencies. The designed multiband antenna with size of 82.05x104.76x1.60 mm^3 was optimized for collecting more energy and then, implemented on FR4 substrate. Return loss, voltage standing wave ratio, and impedance of the manufactured multiband microstrip antenna were measured by vector network analyzer. The multiband antenna gain was calculated as 2.02 dBi. Furthermore, a good agreement was noted between the measurement and simulation results of the multiband microstrip antenna. As a result, it is determined that the produced multiband microstrip antenna is a useful and suitable antenna for RF energy harvesting circuits.

Introduction

Microstrip antenna is a type of antenna that can be produced simply, has a very low cost, suitable for planar and other surfaces, and generally used in wireless communication. Microstrip antennas are commonly utilized in radio reception and transmission systems. This can be attributed to the following reasons: They possess a low profile (their height is significantly less than the operating wavelength); their width and length are small (less than the operating wavelength). [1]-[2]. Due to the development of technology and the requirement for mobile electronic devices, the need for more compact antennas has increased. For this reason, microstrip antennas have started to come to the fore. When microstrip antennas are examined, they have proven to be very good radiators in many applications, but they have different disadvantages compared to other microwave antennas. Numerous research endeavors have focused on enhancing the bandwidth capabilities of microstrip antennas. Some modifications have been reported in the literature to improve and increase the bandwidth or gain of the antennas. E. Levine and at al. investigated radiation and losses in microstrip antennas equipped with a corporate feed network. A surface current approach is employed for the feed lines, similar to ideal transmission lines, while examining the free-field radiation and surface wave excitation of typical segments within the feed networks. An analysis was conducted on a four-element array antenna with a feed network, and the predicted radiation patterns, directivity, and gain were compared against simulation and experimental results. The gain and directivity of large arrays comprising 16, 64, 256, and 1024 elements were computed, with measurements reported in the 10-35 GHz frequency range [3]. A. Elhamraoui and at al. introduced a compact dual-band and miniature microstrip antenna designed for Radio Frequency Identification (RFID) readers. This antenna was developed based on a straightforward defected ground structure employing slots in the ground plane, facilitating its fabrication significantly. The measured outcomes indicated that the achieved impedance bandwidth was 70 MHz and 490 MHz, respectively, which proved suitable for dual-band RFID applications. Furthermore, the

proposed antenna exhibited favorable radiation characteristics, offering a gain increase of 1.1 dBi at 2.45 GHz and 2.8 dBi at 5.8 GHz across two operational bands [4]. There have been several studies on the integration issues of multiband antennas, such as the Tri-band U-slot monopole antenna [5] and the Dual-band compact radiator planar antenna [6]. Modifications aimed at enhancing the antenna bandwidth have been documented in the literature Examples of strategies explored in the literature to expand the bandwidth of microstrip antennas include the utilization of trapezoidal-shaped antennas [7], employing parasitic strips capacitively coupled to the non-radiating edges of square patch antennas [8], incorporating rectangular antennas with their radiating edges gap-coupled to quarter-wavelength short-circuited parasitic elements [9], experimenting with multilayer structures [10], implementing stagger-tuned resonators [11] as well as investigating log-periodic structures, quasi-log periodic structures, among others [12]. The coupled resonator model is an effective technique to increase antenna size, where patches can be aligned in a plane [13]-[14] or stacked vertically [15]-[16]. Currently, in addition to high-accuracy radar systems, multiband antennas are also required for the application of high data rate wireless communications, satellite navigation systems and similar systems. All these problems can be solved by designing multiband antennas. Microstrip patch antennas have become an excellent solution due to their many features and advantages such as low volume, lightness, low cost, and easy integration into systems. However, problems such as narrow bands of the antenna and low gain arise. Therefore, researchers are trying different ways to obtain a compact multiband, high-gain antenna with multiple resonant frequencies for operations in multiple frequency bands. The frequency response of the VSWR value of a microstrip antenna typically exhibits a resonance characteristic [17]. Expanding the operational bandwidth can be achieved through modifications to the antenna's design, such as altering its shape or employing complex emitter configurations. One approach involves incorporating additional passive radiators, which are excited by the current induced by the active radiator's field and connected to the coaxial line [18]. In this study, optimization was performed post the initial design phase of the microstrip antenna. This optimization process involved the modification of the patch by trimming its edges, reducing the ground plane, and puncturing holes in the antenna's patch. Producing a multiband antenna and adjusting the operating bands of this antenna according to the operating frequencies of the RF energy harvesting circuit can enable this antenna to be used for RF energy harvesting.

RF energy harvesting

Electromagnetic energy within the vicinity of the harvesting antenna is dispersed across different spectral bands. The useful frequency band or bands are determined by spectral measurements. According to the measurement results, single-band, multi-band or wide-band antenna designs may be suitable for use in RF energy harvesting systems. Single-band antennas are easy to design and manufacture but may collect less energy than multi-band antennas. Moreover, in the scenario where the energy harvesting circuit is tailored to accommodate multiple frequency bands, it results in an elevation of the output DC voltage level of the RF energy harvester. While a wideband antenna proves to be efficient in collecting power across a broad frequency spectrum, it's noteworthy that antenna gain experiences a reduction as the distance from the central frequency increases [19].

Microstrip antennas

Microstrip antennas, which have become increasingly common recently, are used in many areas. Aircraft and planes, radar systems, satellite communications and remote technologies can be counted as some of these. Another reason why microstrip antennas are preferred is that they are especially suitable for printed circuit technology. These antennas possess a compact design, rendering them appropriate for application on both flat and curved surfaces. Additionally, their fabrication is straightforward and economical, leveraging contemporary printed circuit technology. Additionally, they exhibit mechanical robustness when mounted on hard surfaces and are compatible with MMIC designs. Moreover, the incorporation of structures such as pins and varactor diodes between the patch and the base conductor (ground) enables the design of adaptive elements with variable resonance frequency, impedance, polarization, and pattern [20]. In addition to their benefits, microstrip antennas exhibit several drawbacks. These include low efficiency, limited power handling capability, high quality factor, suboptimal polarization characteristics, inadequate scanning performance, and a notably narrow frequency bandwidth [20].

Microstrip antenna consists of two layers: a conductor, such as copper or gold, and an insulator, such as Rogers or FR4. The upper part is in the form of a patch with length L and width W, the lower part

represents the ground surface, and between them is the electrical insulator with a thickness.

Microstrip antenna patch geometries

When designing microstrip antennas, products with low dielectric conductivity and thick insulating base materials are preferred. These materials allow for high performance microstrip patch antennas. The radiation needed in the antenna is provided with high bandwidth and efficiency, but large patch sizes limit the radiated areas less. On the other hand, it is observed that as the relative permittivity increases, there is a decrease in the efficiency and radiation pattern of the antenna. For all these reasons, the dimensions of the antenna directly affect the performance and other parameters of the antenna [21].

Feeding methods of microstrip antenna

Microstrip patch antennas are fed using various feeding techniques [22]. Among the most common and frequently mentioned in the literature are coaxial feeding, feeding via microstrip transmission line (including inset feed, quarter wave transmission line, and edge feed), aperture coupled feeding, proximity coupled feeding, and coplanar waveguide feed. Suitability of the feeding method to the application method is also very important. Some feeding methods depend on many different parameters. Optimum selection of these parameters ensures optimum performance. Considering all these, feeding methods affect the input impedance and antenna characteristics and stand out as an important design parameter [22].

Analysis models of microstrip antenna

A microstrip antenna consists of a two-dimensional radiating conductive patch embedded in a thin insulating material, thus qualifying as a two-dimensional planar element for analytical purposes. Analysis of microstrip antennas typically involves models based on equal magnetic current distribution at the edges of the patch. There are various models available for analyzing microstrip antennas, with the most important and commonly utilized ones outlined below [23] :

- Transmission Line Model
- Cavity Model
- Full Wave Model

The simplest and therefore most widely used of these models is the transmission line model. This model can also enable the analysis of the physical structure of the antenna. However, the standard error rate and accuracy are higher than other methods and this method may be incomplete in modeling coupling structures. Gap model has higher accuracy compared to transmission line model [23] but it is more complex. In addition to all these, it is more successful in physical analysis such as transmission line model, but this method is incomplete in modeling coupling structures. When all models are evaluated, the model with the most accuracy is the full wave model [23]. The full wave model can be applied to single-piece structures, as well as to finite and infinite antenna arrays, antennas of arbitrary shapes and coupling structures. However, this model is also complex and lacking in physical analysis [24].

Material and method

In this section, the required calculations for the antenna design were made and the HFSS Ansys program was used for simulation. Then, the designed antenna was produced. The parameters of the fabricated antenna were measured using a Vector Network Analyzer (VNA), followed by a detailed analysis of the obtained results.

Microstrip antenna design

The microstrip antenna configuration features two slits separated by a transmission line of length L, with open-circuited ends. Voltage across the width of the patch reaches its maximum, while current is minimized due to the open-ended structure.

To ensure operation in the fundamental mode, the patch length should be slightly less than λ/2, where λ represents the wavelength in the dielectric medium and is calculated as $\lambda_0 / \sqrt{\varepsilon_{reff}}$, with λ_0 being the wavelength in the gap. Eq. 1 can be utilized to determine the patch width (W) [25].

$$W = \frac{c}{2 f_r} \sqrt{\frac{2}{\varepsilon_r + 1}} \quad (1)$$

Here;

c: Speed of light in space

f_r: Operating frequency

ε_r : Relative permittivity

Since all the electric fields from the patch return to the insulator, some of these fields return to the insulator after passing through the air and hence, there will be a small difference in the relative permittivity. The effective relative permittivity (ε_{reff}) is the relative permittivity in an insulator that takes into account the relative permittivity of air.

The ε_{reff} equation is given as follows [26]

$$\varepsilon_{reff} = \frac{\varepsilon_r+1}{2} + \frac{\varepsilon_r-1}{2}\left[\frac{1}{\sqrt{1+\frac{12h}{W}}}\right] \quad (2)$$

Here;

ε_r : Relative permittivity

W: Patch width

h: Insulating material thickness

As the electric field lines propagate through the air, the patch length elongates on both sides. This increase in length, represented by ΔL, can be calculated using the following equation:

$$\Delta L = 0.412h\frac{(\varepsilon_{reff}+0.3)\left(\frac{W}{h}+0.264\right)}{(\varepsilon_{reff}-0.258)\left(\frac{W}{h}+0.8\right)} \quad (3)$$

The effective length, denoted as Leff can be computed using the following equation [24] :

$$L_{eff} = \frac{c}{2f_r\sqrt{\varepsilon_{reff}}} \quad (4)$$

Consequently, the patch's precise length can be computed using Eq. 4 [24]:

$$L = L_{eff} - 2\Delta L \quad (5)$$

When designing a microstrip antenna with a rectangular patch shape, first the substrate material with relative permittivity ε_r, thickness h, and resonance frequency f_r in Hz is selected. In the next step, the dimensions of the antenna are determined according to the desired carrier frequency, that is, the width W and length L of the patch must be determined. At the same time, the feeding method to be used must also be selected. In this study, FR4 epoxy was used as a substrate with relative permittivity ε_r=4.3 and thickness h=1.55 mm. On the other hand, copper was chosen as the conductive material to create the patch and soil surface and the microstrip line feeding method was used. In addition, the designed antenna is required to operate at the carrier frequency of 879.5 MHz. The dimensions of the antenna patch are calculated as follows:

Step 1: The following equation is used to determine the width of the patch on the antenna [25]

$$W = \frac{c}{2\,f_r}\sqrt{\frac{2}{\varepsilon_r+1}} \quad (1)$$

Here, W is the width of the patch, c (3x10^{11} mm/s), f_r (879.5 MHz) is the operating frequency, and ε_r (4.3) is the relative permittivity. For these values, the width of the patch was calculated as (W=104.76 mm)

Step 2: The effective relative permittivity ε_{reff} was determined as (ε_{reff}=4.170) by Eq. 2 [26]

$$\varepsilon_{reff} = \frac{\varepsilon_r+1}{2} + \frac{\varepsilon_r-1}{2}\left[\frac{1}{\sqrt{1+\frac{12h}{W}}}\right] \quad (2)$$

Step 3: From Eq. 3 [26], the incremental length produced by the side fields was calculated as (ΔL= 0.886).

$$\Delta L = 0.412h\frac{(\varepsilon_{reff}+0.3)\left(\frac{W}{h}+0.264\right)}{(\varepsilon_{reff}-0.258)\left(\frac{W}{h}+0.8\right)} \quad (3)$$

Step 4: L_{eff} the effective length of the patch was calculated with Eq. 4 [24], then the actual length of the patch was obtained as L=82.05 mm using Eq. 5 [24].

$$L_{eff} = \frac{c}{2f_r\sqrt{\varepsilon_{reff}}} \quad (4)$$

$$L = L_{eff} - 2\Delta L \quad (5)$$

Bandwidth enhancement techniques

The most significant drawback of microstrip antennas is their narrow bandwidth, typically ranging from 2% to 5%. Consequently, extensive research has been conducted to develop various techniques aimed at expanding the bandwidth of microstrip antennas. The primary objective of these techniques is to address the inherent bandwidth limitation caused by the small electrical volume occupied by the antenna element. Most of these techniques fall into two categories: those utilizing an impedance matching network and those employing parasitic elements [21]. In both scenarios, the double-tuning effect is frequently employed. One method for enhancing the bandwidth of microstrip antennas involves using a thick patch with low dielectric constant in conjunction with a stub tuning network. However, when the matching network is situated in the same plane as the antenna structure, spurious radiation from the matching network can pose a

challenge. The bandwidth of the antenna element is typically governed by impedance variations. Consequently, designing a planar impedance matching network is often feasible to enhance the bandwidth. It's worth noting that the pattern bandwidth is generally much superior to impedance bandwidth. In this manner, bandwidths of 9% to 12% [27] and 15% [28] have been attained for probe-fed and microstrip line-fed elements. Furthermore, a bandwidth of 13% was achieved for the proximity-coupled patch element with the stub tuning network. If the matching network is in the same plane as the antenna element, spurious radiation from the matching network can be a problem. It has been said that when the matching network and the antenna element are in the same plane, radiation from the matching network may be a problem. Therefore, increased bandwidth can be produced by different technic, using a more complicated element shape and using parasitically coupled elements to create a double-tuned resonance. This is best achieved using two stacked patches. Bandwidths ranging from 10% to 20% have been successfully attained using probe-fed stacked patches [29] , while aperture-fed stacked patches have demonstrated bandwidths between 18% and 23% [30], [31].

In line with the principles of broadband antenna design, the process of etching slots onto the radiation patch has been recognized as a viable method to broaden the bandwidth and improve matching characteristics. Consequently, the development of novel antenna designs often includes incorporating fractal slots onto the rectangular radiating patch [32].

In the study conducted by Yanyan Shi and colleagues, it was observed that the length of the ground plane (Lg) has a significant impact on the performance of the proposed antenna. An investigation into the variation of Lg was conducted in their microstrip antenna design. It was found that both the bandwidth and reflection coefficient of the proposed antenna are substantially affected by changes in Lg. As Lg increases, the antenna's bandwidth gradually decreases [32].

Modeling and simulation

In this study, the microstrip antenna design was carried out utilizing the HFSS program [33]. The dimensions of the microstrip antenna were set to ε_r= 4.3 and h=1.55 mm. The patch width was determined as 104.76 mm, and the patch length was set to 82.05 mm, optimized for the 879.5 MHz carrier frequency band. A rectangular microstrip antenna with line feeding method was designed. The final design of the antenna was made by optimizing the dimensions of the patch, feed line and other parameters to find the best value. However, it was necessary to make some adjustments in order to achieve the best results and increase the number of bands and bandwidth of the antenna. As mentioned in previous studies, it was observed that opening slots on the patch and making different arrangements on the patch were effective in increasing the bandwidth and number of bands of the antenna. Based on this, in order to increase the number of bands and bandwidth of the antenna, two triangles were symmetrically cut from the upper right and left corners of the patch, and two triangles were symmetrically cut from the lower right and left edges. Then, a circle with a radius of 15 mm was cut in the middle of the patch. To further optimize the antenna, two more semicircular segments of 15.85 mm radius were cut from the lower right and left edges. All these were not sufficient for the optimization of the antenna, and then some changes were made in the design for optimization purposes by reducing the ground surface. The front and rear views of the antenna designed with the support of HFSS software are shown in Fig. 1 and Fig. 2, respectively. This has led to improving the return loss, increasing the frequency bandwidth and number of bands, and eliminating undesirable frequencies. Additionally, antenna efficiency has also increased.

The characteristics of the designed antenna are detailed in Table 1.

Table 1. Designed microstrip antenna parameters.

Parameter	**Value**
Operating Frequency (f_r)	879.5 MHz
Relative Permittivity (ε_r)	4.3
Insulating Material Thickness	1.55 mm
Patch Width (W_p)	104.76 mm
Patch Length (L_p)	82.05 mm
Width of Feed Line (W_f)	4.8 mm
Length of Feed Line (L_f)	28.98 mm
Width of Ground Surface (W_g, W_s)	116 mm
Length of Ground Surface (L_g)	9 mm

Length of Material (L_s)	100 mm
Radius of Central Circle (R_a)	15 mm
Radius of Side Circles (R_b)	15.85 mm
Distance Between Center Circle to L_p (x)	52.38 mm
Distance Between Center Circle to W_p (y)	21.25 mm
Length of (E_a)	33.26 mm
Length of (E_b)	20.51 mm
Length of (E_c, E_d)	15.85 mm
Length of (E_p)	52.38 mm

The front and back views of the microstrip antenna designed with the HFSS program are shown below in Fig. 1 and Fig. 2.

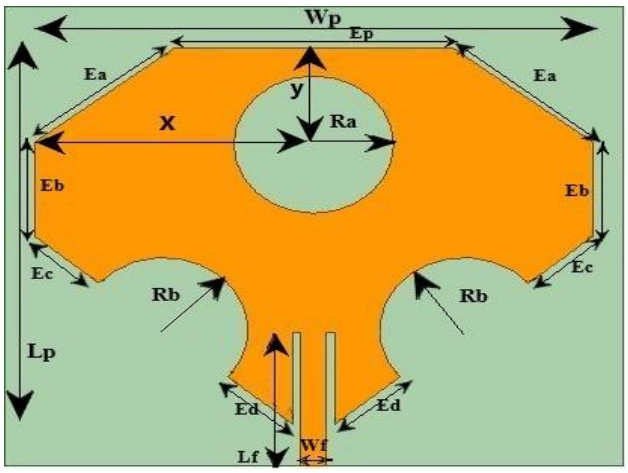

Fig. 1. Front view of the designed antenna

Fig. 2. Back view of the designed antenna

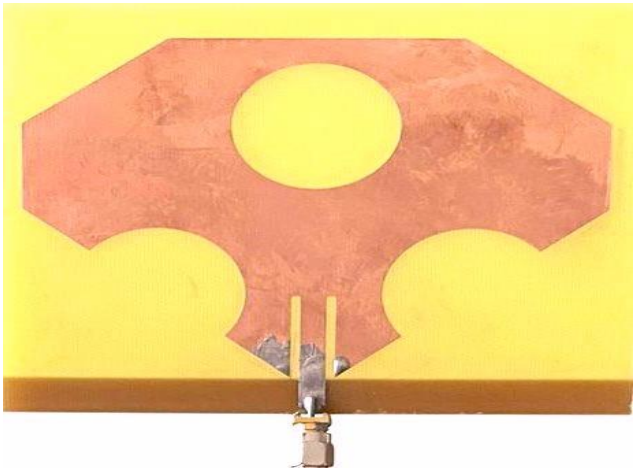

Fig. 3. Front view of the produced antenna

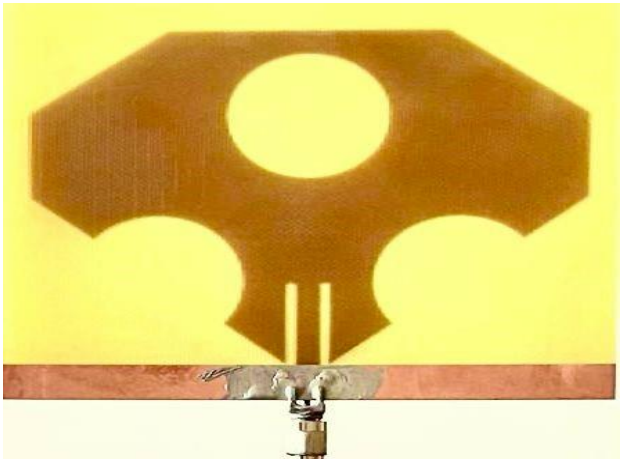

Fig. 4. Back view of the produced antenna

The rectangular microstrip antenna shown in Fig.1 and Fig. 2. was designed using the HFSS Ansys program [33]. Then, this antenna was printed in DFX format using the PCB layout program and produced as seen in Fig. 3. and Fig. 4. using FR4 substrate material.

In this study, VNA which measures in a wide spectrum, was used to measure the S parameters and other parameters. The VNA processes transmitted and reflected waves from a network to show input impedance, RL, VSWR and many other network characteristics. It uses a mathematical error correction/calibration technique. The offering unparalleled performance in a handheld solution for two-port, two-way measurements, this type of device can make very precise circuit measurements even at microwave frequencies [34].

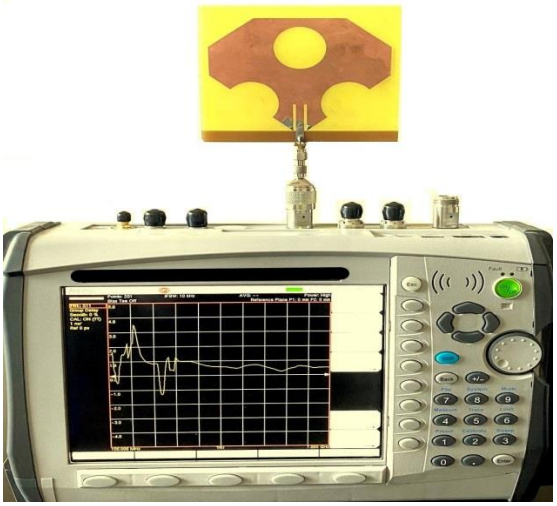

Fig. 5. Vector network analyzer

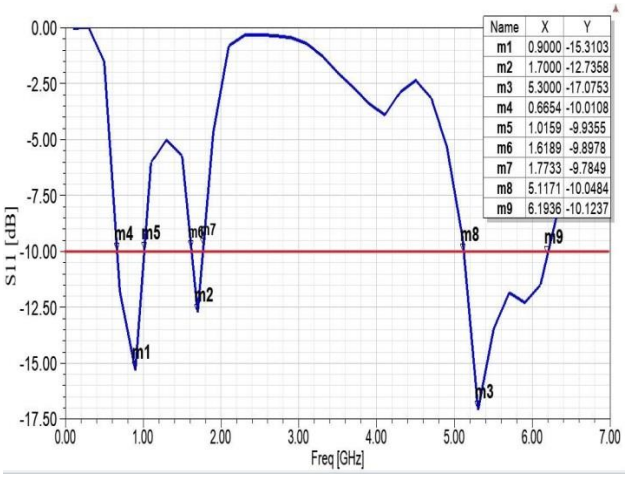

Fig. 6. S11 graph and bandwidths of the designed antenna

Results and discussion

In this study, a microstrip antenna intended to operate in more than one band was designed with the HFSS program. After the antenna design phase, it was manufactured on a low-profile FR4 substrate. The microstrip antenna underwent measurements using a Vector Network Analyzer (VNA), and these measured results were then compared against the simulated data.

Simulation results

S parameter (S11)

In this study, it is seen that the designed antenna operates in three different bands. Upon examining the graph, it is observed that the antenna operates at carrier frequencies of 900 MHz, 1700 MHz, and 5400 MHz. Fig.6. shows the operating frequencies and bandwidths of the antenna in detail. Accordingly, the bandwidth in the first operating band is seen as 350 MHz. When we look at the second bandwidth, it is seen as 154 MHz and finally, the bandwidth of the third band is 1.076 GHz.

The return loss graph of the antenna is seen below in Fig. 6. The return loss of the first band was measured as -15.31 dB at 900 MHz frequency, the return loss of the second band was measured as -12.73 dB at 1.7 GHz frequency band, and the return loss of the third band was measured as -17.07 dB at 5.3 GHz frequency band.

Voltage standing wave ratio (VSWR)

VSWR value is a very important parameter after the microstrip antenna design phase is completed. Looking at the VSWR graph in Fig. 7, the VSWR value is 3.01 at 0.90 GHz, which is the first operating band of the antenna. When we look at the 1.70 GHz frequency band, which is the second operating band of the antenna, the VSWR value is 4.08 and at the 5.3 GHz frequency band, it is 2.44.

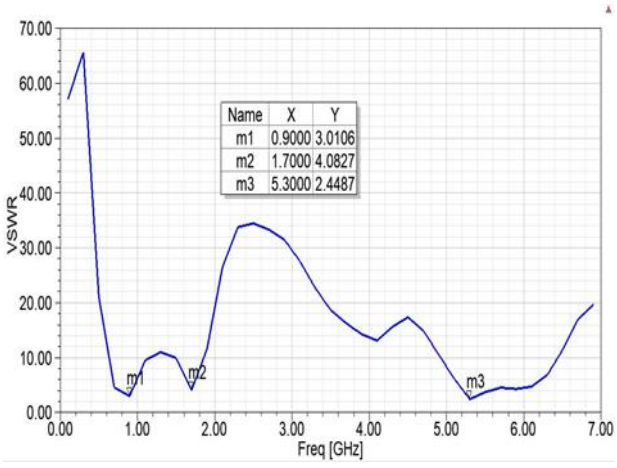

Fig. 7. VSWR graph of the designed antenna

Impedance

Fig. 8 shows the real and imaginary impedance values of the microstrip antenna. Considering the standard 50 Ω, it can be seen in the graph that there is 67.57 Ω at the 0.90 GHz frequency value at point m1, 37.66 Ω in the 1.7 GHz frequency band at point m2, and 47.91 Ω in the 5.3 GHz frequency band.

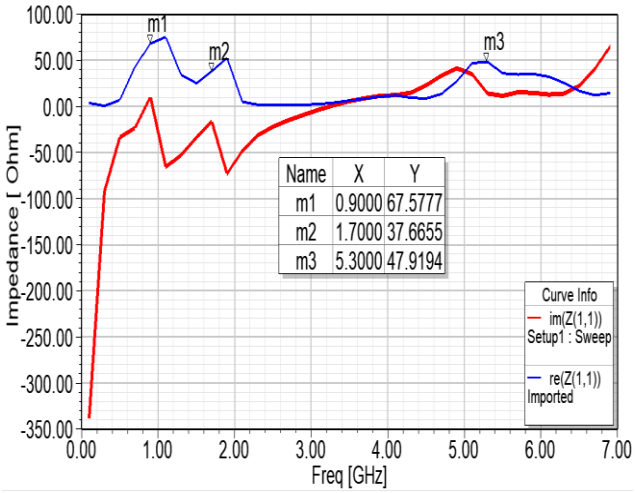

Fig. 8. Impedance graph of the designed antenna

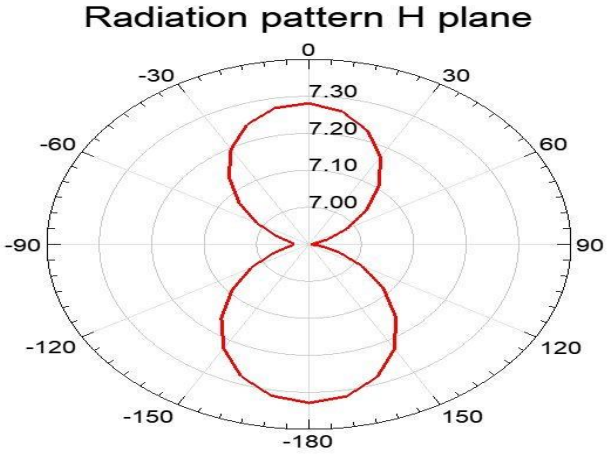

Fig. 10. Radiation pattern H plane

Radiation pattern

Another important parameter of the microstrip antenna is the radiation pattern as shown in the graph below. The radiation pattern of the antenna is plotted at the initial frequency of 879.5 MHz, which is selected as the initial design frequency of the antenna. It is shown in the E plane in Fig. 9. and in the H plane in Fig. 10. The omnidirectional nature in the H-plane suggests that the antenna possesses effective reception capabilities, advantageous for gathering RF energy in space. Moreover, a symmetrical radiation pattern is formed both vertically and horizontally in the H-plane.

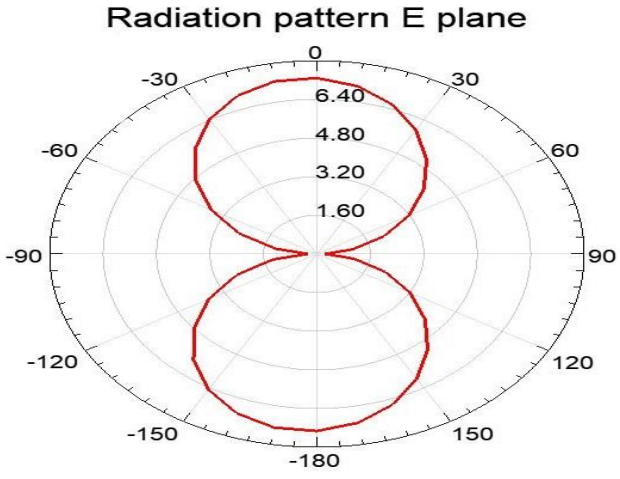

Fig. 9. Radiation pattern E plane

Directivity and gain

The gain and directivity graphs of the microstrip antenna are shown in Fig. 11. The maximum gain and directivity values of the antenna are obtained as 2.02 dBi and 2.33 dBi, respectively at 5300 MHz.

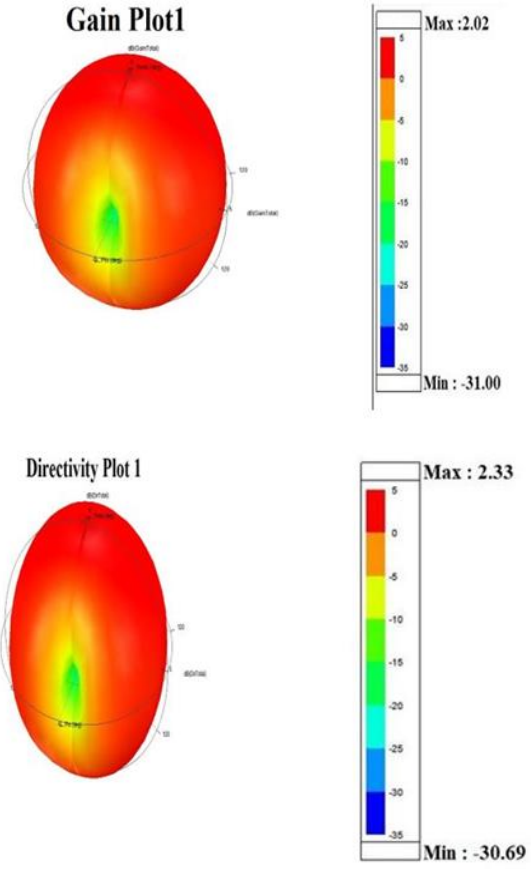

Fig. 11. 3D polar plot gain and directivity of the designed antenna

Comparison of simulation with measurement results

In this study, some parameters of the microstrip antenna were measured by VNA. Then, when the results obtained during the simulation process were compared with the measurement values, the following graphs were obtained.

S parameter

Fig. 12. shows the S parameter graph of the produced microstrip antenna. The m1, m2 and m3 values represent the lowest values of measured return loss. On the other hand, m1, m2 and m3 values are the lowest values of the simulation return loss. The return loss of the first band was simulated as -15.31 dB at 900 MHz frequency, the return loss of the second band was simulated as -12.73 dB at 1.7 GHz frequency band, and the return loss of the third band was simulated as -17.07 dB at 5.3 GHz frequency band.

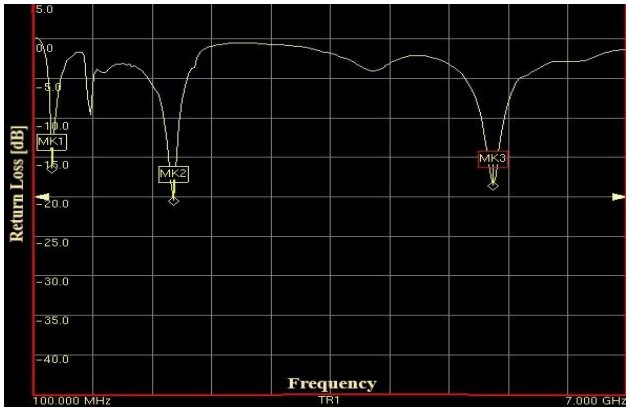

Fig. 12. Measurement result of return loss

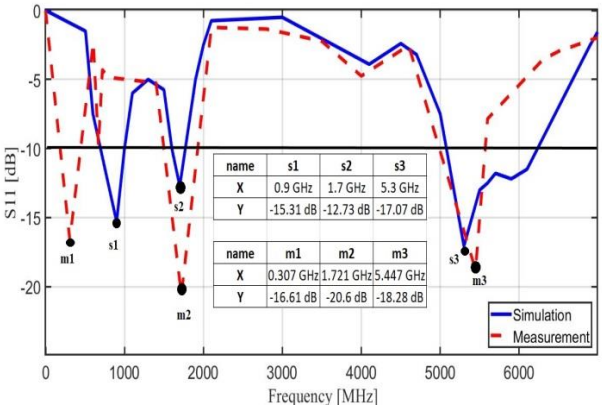

Fig. 13. Comparison of simulation with graphs

When the measurement results of the produced antenna are analyzed, it is seen that return loss values are -16.61 dB in the 307 MHz frequency band in the first marker (m1), -20.60 dB in the 1721 MHz frequency band in the second marker (m2), and -18.28 dB in the 5447 MHz frequency band in the third marker (m3), respectively.

First of all, when we look at the graphs, it can be seen that the curves are generally very similar to each other. Unlike the simulation results, it is seen that the produced antenna operates in four bands. The 307 MHz frequency band was not visible in the simulation results. On the other hand, the 900 MHz frequency band that appeared in the simulation could not fall below -10 dB according to the measurement results. But it is very close. In this respect, there is a difference between the simulation and measurement results. This difference may be due to various reasons, such as small changes in the relative permittivity of the material used, as well as small errors in antenna dimensions or simple manufacturing errors. But, in summary, with the addition of the 307 MHz frequency band, this can be considered a good result since we aim to design a multiband antenna.

Impedance

Below you can see the measurement results of the antenna's impedance values in Fig. 14.

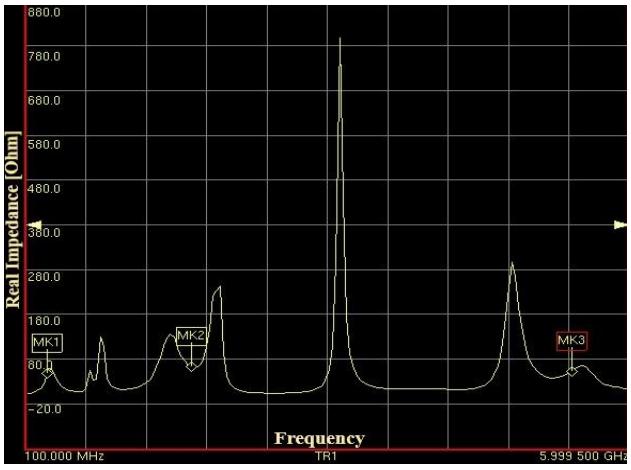

Fig. 14. Measurement result of the real impedance

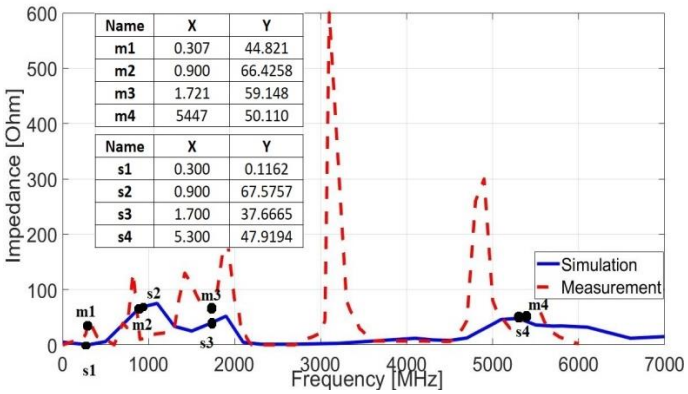

Fig. 15. Comparison of simulation and measurement graphs of impedance

If an antenna is mismatched, power loss can significantly increase because the power generated by the source will be reflected. Input impedance, a criterion related to power, plays a critical role in

determining the power received by the antenna. Therefore, input impedance is an important parameter to consider for ensuring the maximum power transmission from the source to the antenna. Ideally, the input impedance should match the impedance generated by the source [35].

The impedance value in the 307 MHz frequency band, which is not in the simulation but appears in the measurement, was measured as 44.821 Ω, the real impedance in the 900 MHz frequency band was measured as 66.4258 Ω, the real impedance in the 1721 MHz frequency band was measured as 59.148 Ω, and the real impedance in the 5447 MHz frequency band was measured as 50.110 Ω.

VSWR values

When looking at the VSWR values, it can be seen that the graphic curves of the simulation results and measurement results are almost similar. On the other hand, it is seen that there are some differences at the VSWR values in the frequency bands. When the simulated antenna is later manufactured, small differences are observed between many parameters of the simulated and manufactured antenna. These differences are usually due to manufacturing errors. If we recall the previous simulation results; at 0.90 GHz, which is the first operating band of the antenna, the VSWR value was 3.01. When we look at the 1.70 GHz frequency band, which was the second operating band of the antenna, the VSWR value was 4.08. In the 5.3 GHz frequency band, it was 2.44. Accordingly, the VSWR value in the 307 MHz frequency band is seen as 1.38. Secondly, in the 1721 MHz frequency band, this value is 1.21. The VSWR value in the 5447 MHz frequency band was measured as 1.26. When considering the simulation value of VSWR, it is 3.01 at 0.90 GHz, which is the first operating band of the antenna. 1.70 GHz frequency band, which is the second operating band of the antenna, the VSWR value is 4.08 and when we look at the 5.3 GHz frequency band it is 2.44.

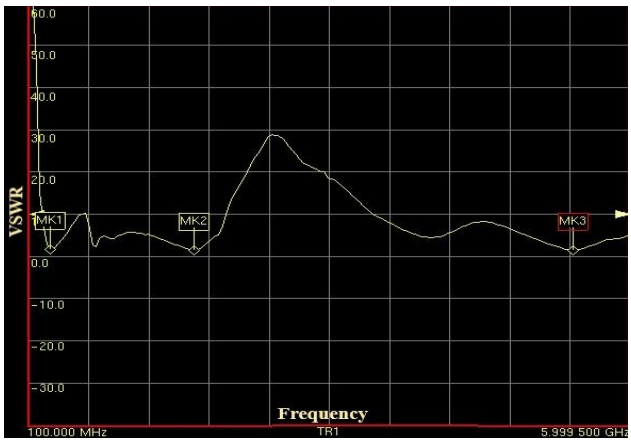

Fig. 16. Measurement result of VSWR

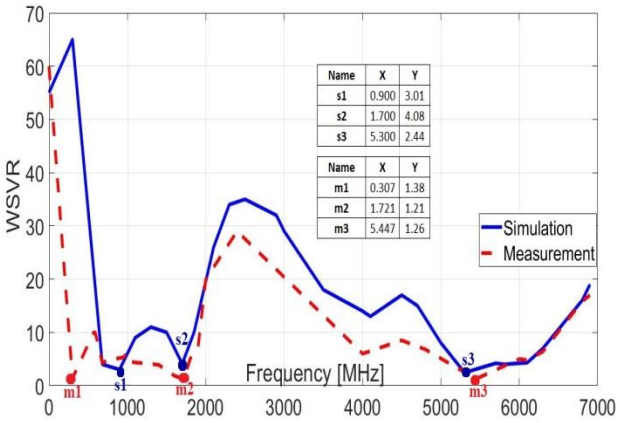

Fig. 17. Comparison of simulation and measurement graphs of VSWR

H. Yousefaalturk and at al. designed a microstrip antenna for RF energy harvesting circuit in the 915 MHz frequency band in 2022. In this study, it was observed that the antenna operated within the frequency range of 830 MHz to 1040 MHz, with a measured bandwidth of 210 MHz [36]. Our designed antenna has several advantages over this antenna. Firstly, our antenna has bandwidths of 350 MHz in the first band, 154 MHz in the second band, and up to 1071 MHz in the third band. Additionally, since our antenna is multi-band and has a wider bandwidth, it can be easily used in many applications. In 2023, Hüseyin Aslan and at al. conducted research on microstrip antenna designs for RF energy harvesting. Several antenna designs were explored in the study. The initial microstrip antenna design operates in the frequency bands of 2300 MHz to 2450 MHz, with a measured bandwidth of approximately 150 MHz. Subsequently, the designs were optimized, and the best-performing design operated in the frequency bands of 2353 MHz to 2446 MHz, with a measured bandwidth of approximately 90 MHz [37]. Compared to the antenna we designed; our design has yielded much better results in terms of bandwidth. Additionally, our antenna, which operates in different frequency bands, also provides advantages for use in various fields.

Conclusions

In this study, a multiband microstrip antenna was designed and then, implemented. The design process for the microstrip antenna commenced with the calculation of dimensions for both the patch and ground. Subsequently, techniques such as opening slots on the patch, and shortening the ground surface (Lg), as mentioned in the literature, were employed to increase the bandwidth and number of bands, aiming to optimize the antenna for our study. The optimization steps were performed intuitively. The ground surface has been reduced to 9 mm to increase

bandwidth and eliminate the undesired frequencies. The ground surface length of 9 mm provided the best bandwidth. Then, triangular pieces were cut from the four edges of the patch and semicircular pieces were cut on the lower right and left edges. Finally, the microstrip antenna, whose dimensions were calculated and optimized, was simulated with the support of the software program.

This triple band microstrip antenna operates at the carrier frequencies of 307 MHz, 1721 MHz and 5447 MHz. In this respect, it is a suitable antenna for triple band RF energy harvesting. When considering the parameters such as return loss, real and imaginary impedances and VSWR values of the produced microstrip antenna, it is seen that there is a good agreement between the simulation and measurement results.

Acknowledgement

This research was supported by Dicle University Scientific Research Projects (Project Number: MÜHENDİSLİK.23.013).

References

[1] B. S. Kranth, G. K. Dilip, and K. Bhagath Kumar, "Planar Patch Antenna for 2.4 GHz Wireless Applications," Ver. II, IOSR Journal of Electronics and Communication Engineering (IOSR-JECE) e-ISSN: 2278-2834, p- ISSN: 2278-8735.Volume 9, Issue 3, Ver. II (May - Jun. 2014), PP 61-64 www.iosrjournals.org. doi:10.9790/2834-09326164.

[2] J. A. Ansari, P. Singh, S. K. Dubey, R. U. Khan, and B. R. Vishvakarma, "H-shaped stacked patch antenna for dual band operation," *Progress In Electromagnetics Research B*, vol. 5, pp. 291–302, 2008, doi: 10.2528/pierb08031203.

[3] E. Levine, G. Malamud, and D. Treves, "A study of microstrip array antennas with the feed network," *IEEE Transactions on Antennas and Propagation, 37:4 (1989)*.

[4] A. Elhamraoui, E. Abdelmounim, J. Zbitou, H. Bennis, and M. Latrach, "A new design of a microstrip antenna with modified ground for RFID applications," *International Journal of Intelligent Engineering and Systems*, vol. 11, no. 6, pp. 44–51, 2018, doi: 10.22266/IJIES2018.1231.05.

[5] H. F. Abutarboush and A. Shamim, "Paper-based inkjet-printed tri-band U-slot monopole antenna for wireless applications," *IEEE Antennas Wirel Propag Lett*, vol. 11, pp. 1234–1237, 2012, doi: 10.1109/LAWP.2012.2223751.

[6] X. L. Sun, L. Liu, S. W. Cheung, and T. I. Yuk, "Dual-band antenna with compact radiator for 2.4/5.2/5.8 GHz WLAN applications," *IEEE Trans Antennas Propag*, vol. 60, no. 12, pp. 5924–5931, 2012, doi: 10.1109/TAP.2012.2211322.

[7] G. Kumar and K. C. Gupta, "Trapezoidal shaped microstrip antennas for wider bandwidth and beamwidth," *Int. Conf. Commun. Circuits and Syst., Calcutta (India)*, p. 7, Dec. 1981.

[8] D. H. Schaubert and F. G. Farrar, "Some conformal printed circuit antenna designs," *in Proc. Workshop Printed Circuit Antennas, New Mexico State Univ.*, vol. 1-, pp. 5.1-5.21, Oct. 1979.

[9] C. Wood, "Improved bandwidth of microstrip antennas using parasitic elements," *Proc. Inst. Elec. Eng., MOA*, vol. 127, no. 4, pp. 231–234, Aug. 1980.

[10] P. S. Hall, C. Wood, and and C. Garrett, "Wide bandwidth microstrip antennas for circuit integration," Electron. Lett., vol. 15, no. 15, pp.," *Electron. Lett.*, vol. 15, no. 15, pp. 458–460, Jul. 1979.

[11] J. H. Pues, Vandensande, and and Van de Capelle, "Broadband microstrip resonator antennas," *in IEEE Antennas Propagat. Soc. Int. Symp. Digest*, pp. 268–271, 1978.

[12] H. Pues et al., "Wideband quasi-log-periodic microstrip antenna," *Proc. Inst. Elec. Eng., MOA*, vol. 128, no. 3, pp. 159–163, Jun. 1981.

[13] G. Kumar and and K. C. Gupta, "Broad-Band Microstrip Antennas Using Additional," *IEEE Trans. Antennas Propag., vol. 32, no. 12*, pp. 1375–1379, 1984.

[14] S. H. Wi, Y. S. Lee, and J. G. Yook, "Wideband microstrip patch antenna with U-shaped parasitic elements," *IEEE Trans Antennas Propag*, vol. 55, no. 4, pp. 1196–1199, Apr. 2007, doi: 10.1109/TAP.2007.893427.

[15] S. D. Targonski, R. B. Waterhouse, and D. M. Pozar, "Design of Wide-Band Aperture-Stacked Patch Microstrip Antennas," 1998.

[16] Nasimuddin and Z. N. Chen, "Wideband microstrip antennas with sandwich substrate," *IET Microwaves, Antennas and Propagation*, vol. 2, no. 6, pp. 538–546, 2008, doi: 10.1049/iet-map:20070284.

[17] R. Z. Wu, P. Wang, Q. Zheng, and R. P. Li, "Compact CPW-fed triple-band antenna for diversity applications," *Electron Lett*, vol. 51, no. 10, pp. 735–736, May 2015, doi: 10.1049/el.2015.0466.

[18] B. R. Piper and M. E. Bialkowski, "Electromagnetic modeling of conformal wideband and multi-band patch antennas by bridging a solid-object modeler with MoM software," *IEEE Antennas Propag Mag*, vol. 46, no. 5, pp. 42–52, Oct. 2004, doi: 10.1109/MAP.2004.1388825.

[19] M. Cansiz, D. Altinel, and G. K. Kurt, "Efficiency in RF energy harvesting systems: A comprehensive review," *Energy*, vol. 174. Elsevier Ltd, pp. 292–309, May 01, 2019. doi: 10.1016/j.energy.2019.02.100.

[20] B. Dökmetaş, "5G Uygulamaları için DGS Kullanılarak Mikroşerit Yapıların Analizi Doktora Tezi," Ankara, Dec. 2021.

[21] D. M. Pozar, "Microstrip Antennas Invited Paper Proceedings of the IEEE," Jan. 1992.

[22] J. R. James and P. S. Hall, "Handbook of Microstrip Antennas," london, 1988.

[23] İ. Ataş, "Yüksek Kazançlı Mikroşerit Antenlerin HFSS ile Modellenmesi ve Tasarımı Doktora Tezi," Dec. 2019.

[24] R. Gang, P. Bhartia, I. Bahl, and A. Ittipiboon, "Microstrip Antenna Design Handbook," 2001.

[25] Constantine A. Balanis, *Antenna Theory and Analysis Design Third Edition*. 2005.

[26] Yi Huang and Kevin Boyle, "Antennas From Theory To Practice," 2008.

[27] H. F. Pues and A. R. Van de Capelle, "An Impedance matching technique for increasing the bandwidth of microstrip antennas.," *IEEE Trans. Antennas Propagat*, pp. 1345–1354, 1989.

[28] J. J. Schuss, J. D. Hanfling, and R. L. Bauer, "Design of wideband patch radiator phased arrays in IEEE Antennas Propagation Symp. Dig," 1989.

[29] A. Sabban, "A new broadband stacked two-layer microstrip antenna in IEEE Antennas and Propagation Symp," 1983.

[30] C. H. Tsao, Y. M. Hwang, F. Kilburg, and and F. Dietrich, "Aperture-coupled patch antennas with wide-bandwidth and dual polarization capabilities," *in IEEE Antennas and Propagation Symp. Dig*, pp. 936-939, 1988.

[31] A. Ittipiboon, B. Clarke, and and M. Cuhaci, "Slot-coupled stacked microstrip antennas," *IEEE Antennas and Propagation Symp. Dig*, pp. 1108–1111, 1990.

[32] Yanyan Shi, Jianwei Jing, Yue Fan, Lan Yang, Yan Li, and Meng Wang, "A novel compact broadband rectenna for ambient RF energy harvesting," *International Journal of Electronics and Communications*, pp. 264–270, Aug. 2018.

[33] "HFSS Ansys. Accessed: Nov. 16, 2023. [Online]. Avaible: https://www.ansys.com/products/electronics/ansys-hfss".

[34] "Anritsu MS2028C. Accessed: Oct. 9, 2023. [Online]. Avaible: https://www.anritsu.com/en-US/test measurement / products / ms 2028c".

[35] W. L. Stutzman and G. A. Thiele, "Antenna Fundamentals and Definitions," *New York: John Wiley &Sons, Inc*, 1998.

[36] H. Yousefalturk and M. Cansiz, "Design and implementation of microstrip antenna at 915 MHz carrier frequency for RF energy harvesting," *Dicle University Journal of Engineering*, vol. 13, no. 3, pp. 531–538, Sep. 2022, doi: 10.24012/dumf.1150600.

[37] H. Aslan, "RF Enerji Hasatlama İçin Mikroşerit Anten Tasarımı Uygulamaları Yüksek Lisans Tezi," Batman, Nov. 2023.